JAAS
Journal of Analytical Atomic Spectrometry

Micro and Surface Analysis in Art and Archaeology†

Plenary Lecture

F. ADAMS*, A. ADRIAENS, A. AERTS, I. DE RAEDT, K. JANSSENS AND O. SCHALM

University of Antwerp, Department of Chemistry, Universiteitsplein 1, B-2610 Antwerpen, Belgium

A variety of instrumental analytical techniques can be applied to the physical and chemical examination of works of art and archaeology. In this paper, a few examples are discussed of the application of micro-analytical chemistry in this interdisciplinary field. The following subjects from the experience of our laboratory, in collaboration with several specialized institutes, were selected: Early Bronze Age ceramic crucibles, residues and powders from Göltepe, South Central Turkey, have been analysed using surface analytical techniques to investigate potential evidence of tin smelting. The study indicates that the crucibles were used for processing of tin and gives clear evidence of a local tin industry. Roman glass from a collection of objects discovered in Qumrân near the Dead Sea was used to study the corrosion of glass objects in a particularly stable environment over a period of nearly 2000 years. The corrosion of a series of glass-in-lead windows from St. Michael and St. Goedele's Cathedral, Brussels, was studied using electron probe microanalysis and micro X-ray fluorescence. New views can be formulated on the corrosion mechanism, which appears to be a complex multiphase process under the influence of atmospheric pollution. A few preliminary results are discussed for the analysis of glass paintings, in particular carnation red glass paints.

Keywords: *Microanalytical techniques; surface analysis; art objects; archaeology*

Nowadays, a variety of analytical techniques can be applied to the physical and chemical examination of works of art and archaeological objects. In this paper, a few examples of the application of a number of trace and microscopical techniques (X-ray fluorescence analysis, electron probe microanalysis and secondary ion microscopy) will be discussed in order to illustrate the possibilities of microanalytical chemistry in this interdisciplinary field. All the techniques evolved from the laboratory experience acquired in the Micro and Trace Analysis Centre (MiTAC) of the University of Antwerp. The main goal of this research group involves development of methods for trace and microchemical analysis and application of these methods in environmental chemistry and materials science.

In basic analytical chemistry, MiTAC has access to a number of different analytical methodologies in trace analysis and microscopical analysis. These are summarized in Table 1. In addition, the laboratory has access to a number of other methodologies, in other laboratories, for its applied research. We refer to other publications for the details on all these techniques.

In general, hardly any applied analysis depends on the application of a single analytical tool. Very often, it is by the application of a wide range of techniques, and the synergy of answers that they provide, that complex problems can often be readily solved. Archaeological applications require an important arsenal of instrumental tools for the often very complex materials to be studied. Archaeology and analysis of art objects were added to this list of application areas of MiTAC fairly recently. Indeed, the laboratory had acquired some interest in this particular applied research area at the beginning of the 1980s but it was only in the last few years that a more systematic development of this particular research endeavour was beginning to be explored.

This paper describes a number of different recent applications of trace and microscopical analysis in art and archaeology.

EARLY BRONZE AGE ARTEFACTS FROM TURKEY: AN APPLICATION OF SURFACE ANALYSIS IN ANCIENT METALLURGY

This section demonstrates the use of micro and surface analysis methods for the study and analysis of ancient metallurgical artefacts. The project that will be considered runs in collaboration with The Oriental Institute in Chicago. It concerns the excavation of a mining complex containing tin ore and an associated production/habitation site in South Central Turkey. Both sites have been dated to the Early Bronze Age (3000–2200 BC).

The analysed samples originate from the production site in Göltepe. Excavations have disclosed pit house structures, which were filled with debris of a similar nature: grindstone tools, ceramic crucibles, powdered materials, ore fragments and charcoal. It is presumed that these materials are related to roasting and smelting activities of cassiterite from the mine in Kestel.[1] The mine is the first tin mine to be located in Turkey. Until the discovery, it was solely believed that the tin used for producing bronze in Anatolia during the Early Bronze Age was imported from distant places, such as Afghanistan. The tin in the mine, however, is not obvious as the cassiterite is only low grade ore, presumably a remainder of richer deposits. This raises the question of whether the mine was once a productive metallurgical site.

In order to expand the archaeological evidence for a tin industry, the present study focuses on the analysis of a set of residues, crucible fragments and powders from Göltepe. Using several analytical techniques such as electron microprobe X-ray analytical (EPXMA), secondary ion mass spectrometry (SIMS) and X-ray fluorescence (XRF), our intention was to examine whether any remains of tin smelting activities could be found. This work is related to other investigations, in which the issue is approached from a different angle.[2,3]

Residues

One of the crucible fragments excavated contains on its inner surface a distinct visible layer of shiny accretion (a few square centimetres). The matrix of this residue, which basically

† Presented at the Eighth Biennial National Atomic Spectroscopy Symposium (BNASS), Norwich, UK, July 17–19, 1996.

Table 1 Instrumental techniques used at MiTAC

Instrumental trace analysis—
Spark source (Jeol JM 1-BM2, 1974) and glow discharge (VG 9000, 1989) mass spectrometry
Energy-dispersive (Tracor 5000, 1985) and glancing angle wavelength dispersive X-ray fluorescence analysis (Philips prototype, 1995)
Instrumental neutron activation analysis
ICP (Perkin-Elmer 6500 XR, 1982) and microwave-induced plasma optical emission spectrometry
Atomic absorption spectrometry (Perkin-Elmer 5100, 1988)

Microscopical analysis—
Scanning electron microscopy and electron probe microanalysis (Jeol 733, 1983, and Jeol JSM 6300, 1993)
Laser microprobe mass spectrometry (FTMS) (Bruker Spectrospin, 1992)
Dynamic and (soon) static secondary ion microprobe analysis (Cameca 4F, 1985, and TOF-SIMS IV)
Microscopical X-ray fluorescence (laboratory source based on Siemens rotating anode tube)
Micro X-ray fluorescence with synchrotron radiation sources (at different sources)
Scanning transmission electron microscopy (Jeol 1200, 1988) and electron energy loss spectrometry (Zeiss ESI 902)
FT infrared microscopy, scanning Auger microscopy, X-ray photoelectron spectrometry, particle induced X-ray emission (through collaboration)

consists of an iron–calcium–tin–alumina silicate (FeO–CaO–SnO_2–Al_2O_3–SiO_2), contains two types of crystals (Fig. 1). The equiaxed crystals are iron–tin oxides, with an average size of roughly 10 μm^2. Some of these crystals contain small inclusions (a few micrometres in diameter), which appear to be a different type of iron–tin oxide phase, with a higher concentration of tin. The longitudinal crystals are composed of SnO_2. These crystals are 0.5–2 μm wide and can be up to 50 μm long. The two types of crystals are primarily slag minerals originating from the ore and gangue, which have been trapped in the matrix. The results indicate that the residue corresponds in composition to a metallic tin slag.[4] These conclusions were verified by comparing the material in detail with a typical tin slag from Cornwall.[5]

Ceramics

Most of the samples on the site, however, do not show any visible indication of tin residues. Many crucible fragments have been found which possess a smooth grey interior surface, of which it is nevertheless believed that they were used for roasting or smelting cassiterite.

In order to analyse these samples, the crucible sherds were cross-sectioned and embedded in epoxy resin. Electron microprobe analyses have shown that the body of these ceramic materials mainly consists of alumina silicates with fragments of quartz and iron oxides. The inner surface of some crucible fragments contains an accretion layer of $CaCO_3$ of roughly 200–500 μm in thickness, the presence of which is most probably due to the prolonged burial of the material. This layer does not cover the entire inner surface but is observed at localized areas on the surface with varying thickness. Between the $CaCO_3$ layer and the ceramic material a layer of silicate material exists, of which its matrix contains 2–3% tin oxides. This layer can clearly be observed in the back-scattered electron image of a crucible cross-section (Fig. 2), where it is represented by a bright band several micrometres thick. This material contains small inclusions, which appear to consist of a different silicate phase with up to 65% of tin oxides.

In addition, line scans with SIMS were performed across the cross-section of the crucible fragment. In these experiments, the bombarding ion beam is moved across the sample in distinct steps of 10 μm, covering roughly 800 μm in total. At each ion beam position on the crucible, compositional data of the sample are acquired. Fig. 3 shows the results, in which the signals of Ca^+, Sn^+ and SiO^+ are plotted as a function of distance. The left-hand side of Fig. 3 portrays the edge of the sample with the epoxy resin, the right-hand side the bulk of the crucible material. Between, the Ca signal can be observed originating from the $CaCO_3$ layer. The SiO signal is present in the ceramic material, but is also observed in the $CaCO_3$ layer. Again, a tin peak is clearly present at the interface of

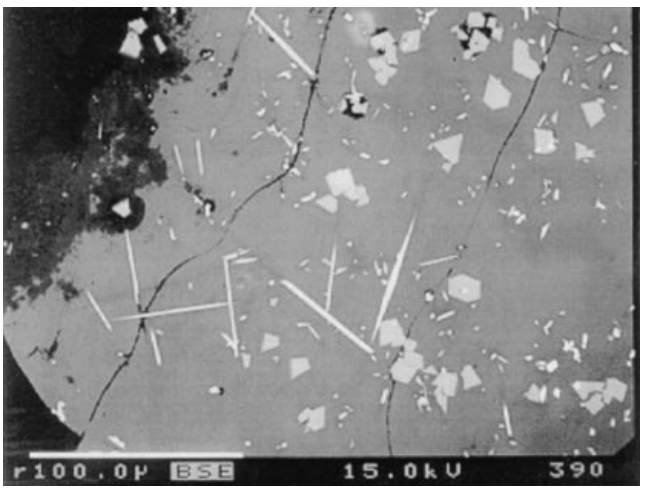

Fig. 1 Back-scattered electron image of accretion material. Tin oxide crystals (longitudinal) and iron–tin crystals (equiaxial) are visible in an alumina silicate matrix. Magnification, ×390. Scale bar, 100 μm.

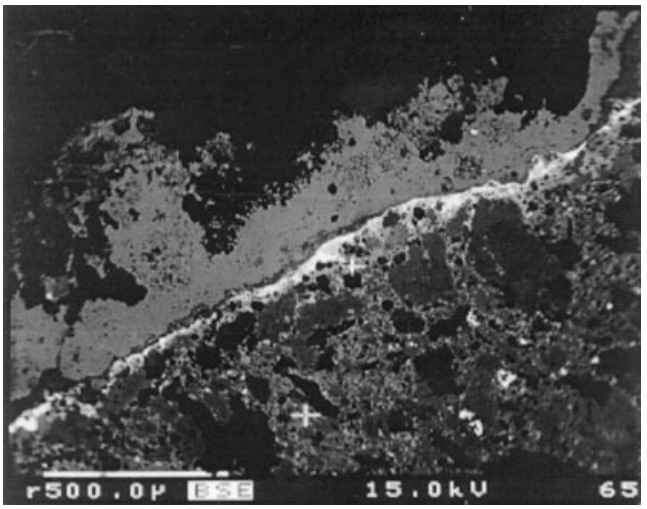

Fig. 2 Back-scattered electron image of a crucible cross-section. The tin-bearing layer is represented by the bright band a few micrometres thick across the image. The dark grey material beneath the layer containing tin is the ceramic material (alumina silicates). The bright spots within the ceramic are iron oxides. The darker areas in the ceramic material are quartz fragments. The medium grey amorphous structure above the tin-bearing layer is the $CaCO_3$ layer. The black area on the upper side of the image is epoxy resin. Scale bar, 500 μm. Magnification, ×65.

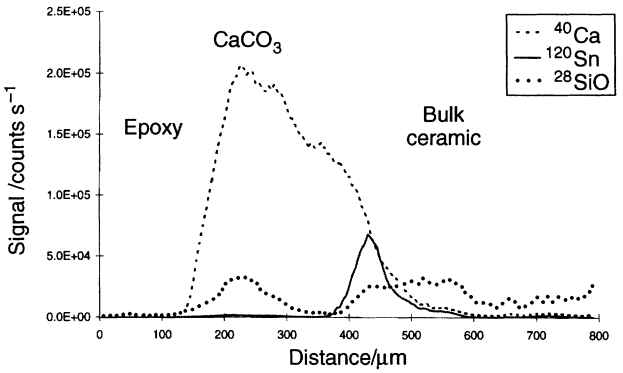

Fig. 3 SIMS line scan of crucible cross-section. The measurement starts on the epoxy resin (left) and is performed towards the body of the ceramic, crossing the $CaCO_3$ and the tin-bearing layer. The absolute signals of Ca^+, SiO^+ and Sn^+ are plotted as a function of distance. The left-hand side of the figure portrays the edge of the sample, the right hand side the bulk of the crucible material.

the ceramic material and the $CaCO_3$ layer and, therefore, at the inner surface of the crucible fragment.

Powders

The pit house structures in Göltepe have also yielded dense concentrations of variously coloured ground ore powders, often in excess of 10 kg. The colours range from purple/burgundy, pink to beige and black and are readily distinguished from the surrounding soil. The powders were analysed mineralogically and found to be the same as material from the Kestel mine.[6] The site of Göltepe contains no mineral bearing veins and analysis of the host rock shows no resemblance to the archaeological material. The latter thus establishes the idea that the materials were taken to the site from their source a few kilometres away.[6]

The powders have been located in ceramic cups, apparently meant for storage, as deposits on the floor in the neighbourhood of hearths and pots, and in garbage dumps. It is assumed that the powdered materials are in turn related to the tin processing that was occurring at the production site. The hypothesis is that some of these powders may be unprocessed ground ore material, while others may be the residue from an ore concentration process (the enriched portion having been extracted) and a third group may be waste materials such as metallic slags.

The intention, therefore, was to perform a further characterization of the powders using XRF and electron microscopy. Bulk analyses were performed using XRF to obtain a general idea of the composition of the samples. Table 2 shows the XRF results of the main elements in nine different powders and show a significant difference in composition. The amount of tin ranges between 0.3 and 2.9%, which is much higher than for similar material found at the Kestel mine (0.07% in hematite samples).[3] The latter suggests that only high tin-containing materials were selectively transported to Göltepe for ore dressing and smelting.[3]

Table 2 XRF results of Göltepe powders (concentration in % m/m)

Sample	Ca	Si	Fe	As	Sn
MRN 2298	9.34	20.45	24.31	0.43	0.28
MRN 2836	2.10	2.55	54.40	0.09	0.85
MRN 3032	9.70	22.77	16.60	0.05	0.34
MRN 3697	7.30	15.04	33.10	0.22	0.64
MRN 3738	4.90	17.84	28.90	0.15	0.70
MRN 3830	7.30	11.02	41.00	0.33	1.18
MRN 3834	15.80	22.06	6.90	0.66	0.43
MRN 3858	7.60	18.15	34.30	0.10	0.85
MRN 4573	4.20	9.10	21.80	0.08	2.93

It is further believed that there is a correlation between the concentration of tin in the powders and their site context. This still needs to be investigated in detail, but there are already a few significant indications.

Sample MRN 2298 for instance was recovered from a garbage dump, a place where one would expect samples to be the least rich in tin. From Table 2, it can be observed that the tin concentration of this sample is significantly lower than that of the other samples. Samples MRN 3834, MRN 3858 and MRN 3830 are three samples which have been located in the same pit house structure, but in different ceramic pots next to each other, presumably meant for storage. In addition, the tin content varies between the three samples, indicating that that samples may represent different stages from an ore concentration process. Sample MRN 4573 contains 2.93% Sn, which is, to date, the highest tin concentration encountered in powdered material from the sites. Sample MRN 3697 has been located next to a hearth in a pit house. The material is strongly magnetic, indicating the presence of magnetite. Experiments have shown that whenever hematite (α-Fe_2O_3) is heated above a temperature of 550 °C, it is partially converted to magnetite (Fe_3O_4) through a maghemite phase (γ-Fe_2O_3).[3] It is, therefore, clear that the magnetically attracted material found in Göltepe is a by-product of a heating process.

This is confirmed by electron microscopy analysis of MRN 2836, which is also highly magnetic. The sample is dark brown to black, again indicating the presence of magnetite. The main purpose of the analyses using electron microscopy is to characterize the particles containing tin. As the cassiterite is located in a hematite-rich environment, iron is likely to be reduced to some extent, which will give rise to a range of iron/tin compounds, called hardhead. Particles composed of Fe and Sn therefore form an additional pointer to heating processes. In addition to SnO_2 particles, MRN 2836 shows the presence Fe–Sn particles (Fig. 4), indicating that the sample is very likely to be a product of roasting or smelting processes.

Conclusions

The present analyses have revealed the presence of tin at the interior surface of the crucible fragments, indicating that these ceramics were probably used for the processing of tin-bearing materials. The fact that the composition of the crucible residue corresponds to a metallic tin slag gives additional evidence for potential tin smelting activities. In addition, some of the

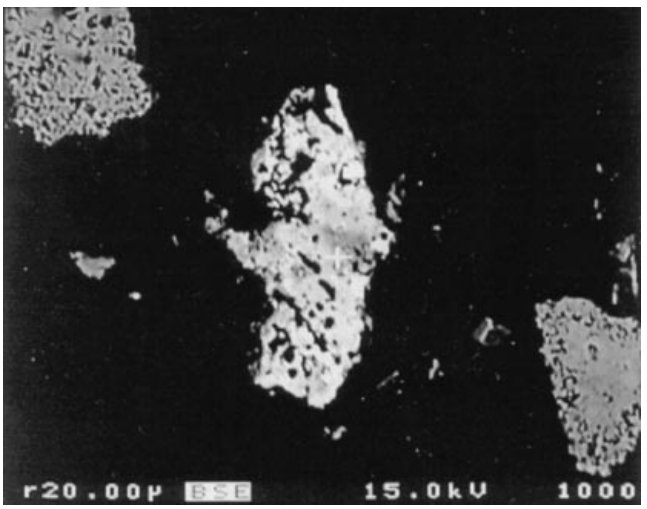

Fig. 4 Back-scattered electron image of a powder particle composed of iron and tin.

powders show sufficient evidence of being heated and confirm the hypothesis that they are, therefore, metallurgical waste materials.

In conclusion, all data provide positive evidence for tin smelting activities at Göltepe. The results of the present study are directly related to investigations involving the search for ancient tin production in Turkey and metal trade during the Early Bronze Age in the Near East.

APPLICATIONS OF MICROANALYTICAL TECHNIQUES TO THE ANALYSIS OF HISTORICAL GLASS AND JADE

Glass, a material of interest to archaeologists, is rarely found in its original state. It has usually been altered by different external factors over a long period of time. Its state of preservation also depends on its own nature. Roman and medieval glass, for example, differ profoundly with respect to their chemical composition. The chemical durability of medieval glass, for instance, decreases due to the use of potash as a raw material instead of soda, which was used in ancient times.[7]

Determination of the composition of various glass samples using EPXMA and micro-synchrotron radiation induced X-ray fluorescence (μ-SRXRF) can reveal information on the provenance and history of objects or windows and/or the site in which they were found. In addition, the correlation with the present day appearance can be studied. In this section, two applications of trace analysis and microanalysis to the characterization of ancient glass will be described: a Roman glass collection from Khirbet Qumrân and medieval glass windows from St. Michael and St. Goedele's Cathedral in Brussels.

Investigation of Glass Objects from Qumrân

In addition to an extensive series of terra-cotta oil lamps and a collection of stone objects, a group of 90 fragments of various glass objects was also recovered during the excavations of Khirbet Qumrân. This archaeological site consists of a collection of ruins of various buildings situated at the eastern edge of the Judean desert, on the north-western shore of the Dead Sea in Israel. It used to be a Roman settlement in ancient times. The glass objects are assumed to date back to the period 4–68 AD. They show corrosion phenomena on their surface due to contact with water in the soil for about 1900 years.[8]

Analysis of the bulk glass

EPXMA and microscopical XRF were applied to the analysis of the bulk glass. All quantitative results of the Qumrân bulk glass were kept together and hierarchical cluster analysis was employed to emphasize the structure in the data. The resulting dendrogram, obtained on the basis of both major and trace element composition (only 36 samples), is shown in Fig. 5. A clear distinction between a large and a small group can be observed. There seems to be no straightforward correlation between the structure in the dendrogram and the typology of the objects except for the fact that the small group is exclusively composed of ointment vessels and goblets.

The difference between these two groups becomes much clearer when the average composition within each group is calculated. In Table 3 the major composition is listed together with the corresponding standard deviation found in each group. The glass is clearly natron-based. Natron is a deposit from the Wadi Natrûn (Egypt) which was extensively used in ancient times for glass manufacture.[7] In the major element composition only the CaO abundance exhibits a significant difference between the two groups.

When the trace element composition is considered (Table 4), a much clearer distinction can be made, more specifically in

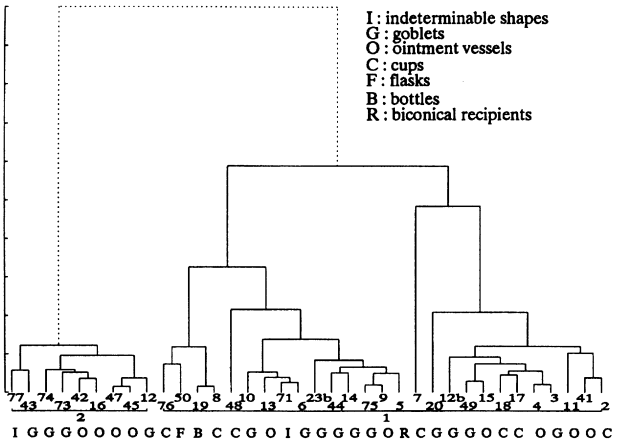

Fig. 5 Hierarchical cluster analysis dendrogram obtained on the basis of both major and trace element composition.

Table 3 Average major element composition of two groups of Qumrân glass samples as determined by SEM (all values in % m/m)*

	Group I	Group II
Na_2O	16.5±0.5	17.0±0.5
MgO	0.2±0.1	0.1±0.1
Al_2O_3	2.5±0.1	2.4±0.3
SiO_2	69.6±0.7	71.6±0.8
P_2O_5	0.1±0.04	<0.1
SO_3	0.1±0.1	0.2±0.1
Cl	0.8±0.1	1.1±0.1
K_2O	0.8±0.1	0.6±0.1
CaO	8.4±0.5	5.9±0.8
TiO_2	0.1±0.02	<0.1
MnO	0.4±0.1	0.8±0.3
Fe_2O_3	0.5±0.1	0.4±0.1

* Significant differences between groups I and II are underlined.

Table 4 Average trace element composition of two groups of Qumrân glass samples as determined by μ-SRXRF (all values in ppm by mass)*

	Group I	Group II
Cr_2O_3	22±5	30±20
NiO	8±1	9±4
CuO	143±36	13±9
ZnO	32±21	19±7
Rb_2O	12±2	12±2
SrO	595±99	540±38
Y_2O_3	9±2	7±2
ZrO_2	86±13	71±9
Mo_2O_3	3±2	2±2
SnO_2	117±33	52±29
Sb_2O_5	281±127	17±26
BaO	165±56	129±56
Ta_2O_5	18±3	3±3
PbO	128±26	16±14

* Significant differences between groups I and II are underlined.

the concentrations of CuO, PbO, SnO_2 and Sb_2O_3. In addition, the trace element signature of each sample within a group is almost identical. This strongly indicates that all objects in one group originate from the same batch of bulk glass and even the two groups seem to be closely related.

Regarding the question of provenance of the objects, the composition information discussed above suggests that almost all objects found at Qumrân were either made locally from the same batch of glass or imported ready-made in large numbers from elsewhere. In either case there seems to have been a relatively large demand for glass vessels of various types, which appears to be consistent with the hypothesis that at this place

some industrial activity in the field of perfume manufacture was located, as suggested in ref. 8.

Corrosion behaviour

Secondary electron images of polished cross-sections of the Qumrân samples show three well defined regions in the glass: a central part of unaffected glass, a leached layer which has formed on the inside of the original glass pane and a precipitation crust on top of the surface. EPXMA maps taken across such cross-sections show marked changes in composition between these different areas.

Overall, the leached layer is depleted in elements such as Na and Ca whereas Al and K are more concentrated in that part, the Si-level is almost the same throughout the whole glass and Mg rises gradually towards the surface. The increase in K in the leached layer is unusual but may be related to the high concentration of this element in the soil the glass had been buried in. The crust is very rich in Ca, which might point to the presence of $CaCO_3$ or $Ca(HCO_3)_2$.

Inside the leached layer, the precipitation of an almost black substance rich in Mn, assumed to be MnO_2, is sometimes observed.[9] In order to obtain a better insight into the migration of various elements between the glass and the surrounding soil, trace element distributions of such an area were also observed. A number of μ-PIXE (micro-particle induced X-ray emission) maps are shown in Fig. 6. Broad alternate bands enriched in different elements can be observed. Since the order and relative thickness of these sub-layers vary considerably among the different samples, it is still very hard to understand all the processes taking place during leaching.

Investigation of Glass Fragments from Thirteenth Century Oculi from Brussels' Cathedral

During the restoration of the choir of St. Michael and St. Goedele's Cathedral in Brussels some round gaps were found in the backwall of the triforium. Many of these gaps contain their original glass windows. These glass windows, initially used for the lighting of the choir, probably date back to 1273, the year when the gallery of the triforium was built. However, they lost their original function during the sixteenth century, when the roof of the gallery was heightened by the building of two chapels.[10–12] All glass panels are severely weathered on both sides. The lightly pitted glass surface is covered with an opaque crust. A thorough study of the chemical composition of the glass and corrosion products and of the durability is necessary to consider further treatment of the glass windows.

Analysis of the bulk glass

Two glass windows, IVB and VIA, each consisting of multiple panels, were analysed. Five panels of each glass window were sampled. EPXMA measurements on polished cross-sections of the 10 glass samples reveal that all glass samples are potash glasses with compositions that are broadly similar. In Table 5 the average chemical composition of five samples taken from window IVB and of five samples taken from window VIA is summarized. However, several factors point to the use of recycled glass: the use of large pieces of uncut glass covered with lead frames, the fact that many panels have a different shade of green and the presence of panels with unfinished grisaille paintings. Principal component analysis (PCA) was

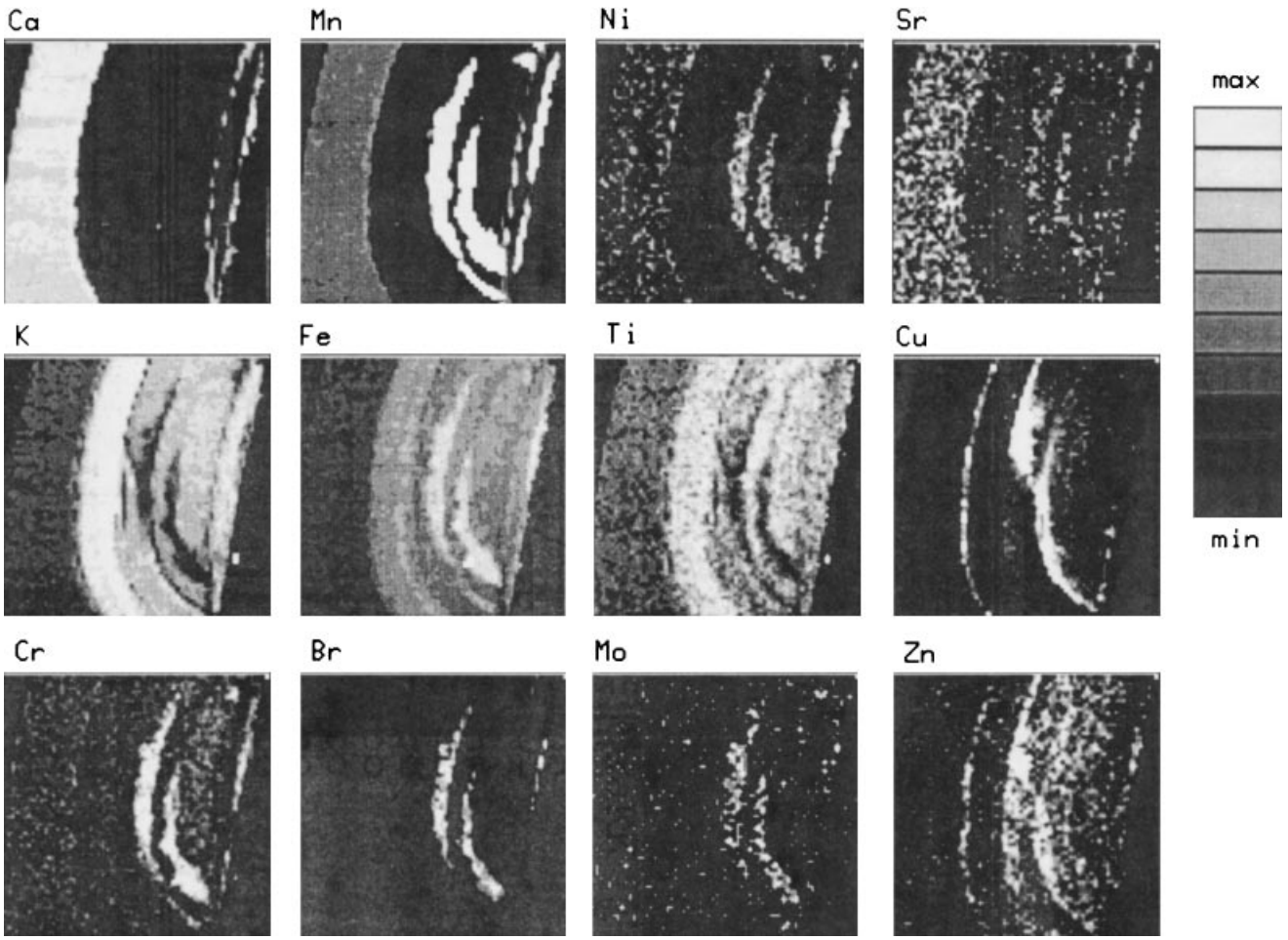

Fig. 6 μ-PIXE maps from a 1200 × 1200 μm region of the corrosion layer with a clear MnO_2 deposit on one of the Qumrân samples.

Table 5 Average major and trace element composition of the bulk glass belonging to two glass windows, IVB and VIA, from Brussels' Cathedral as determined with SEM and μ-SRXRF

	Glass window 1					Glass window 2				
	IVB1	IVB2	IVB3	IVB4	IVB5	VIA1	VIA2	VIA3	VIA4	VIA5
Major element composition (% m/m):										
MgO	5.46	4.98	4.57	4.40	3.94	3.90	3.85	4.28	3.55	3.49
Al_2O_3	4.05	3.42	3.82	3.63	3.93	3.98	4.01	3.04	1.20	1.55
SiO_2	47.25	46.20	46.47	46.29	47.42	47.70	48.33	48.12	52.19	47.96
P_2O_5	2.05	2.23	1.94	1.87	1.17	1.73	1.18	2.52	4.94	1.57
K_2O	11.57	12.21	11.48	11.69	12.41	11.95	12.23	14.62	13.78	19.21
CaO	27.49	28.89	29.31	29.73	28.39	28.16	27.77	25.67	23.44	23.70
MnO	1.07	1.14	1.18	1.21	1.48	1.24	1.43	0.90	0.32	1.92
Fe_2O_3	0.54	0.44	0.58	0.54	0.67	0.60	0.64	0.54	0.54	0.46
BaO	0.52	0.50	0.62	0.65	0.58	0.74	0.57	0.31	0.04	0.14
Trace element composition (ppm):										
TiO_2	1503	1336	1670	1837	1670	1837	1503	1336	1002	1169
NiO	42	35	36	36	39	33	43	29	8	26
CuO	98	218	96	97	100	101	126	211	87	163
ZnO	123	158	163	162	163	127	167	197	270	388
Ga_2O_3	7	5	5	5	7	5	8	4	—	4
Rb_2O	291	318	286	291	368	271	501	438	132	427
SrO	2478	1888	2714	2832	2360	2360	3422	1888	1062	1652
Y_2O_3	15	6.35	—	12	7	10	13	10	7	14
ZrO_2	265	128	234	257	199	240	362	163	100	160
PbO	32	100	41	24	80	36	19	100	23	383

performed to detect glasses of different origin. Fig. 7 shows a Ca–Mn plot since Ca and Mn are highly correlated with PC1 and PC2. All other major elements show a similar correlation. From these plots, samples VIA5, VIA4 and VIA3 are distinguished as outliers. The difference in major element composition confirms the statement of the use of recycled glass. The seven other panels have the same composition and are probably made from the same glass batch. The placement of the windows at a significant height, the cost of glass in the thirteenth century and the function of the oculi as sealers, allowing light to get through, explain why recycled glass was used.

Description of the weathered surface

The seriously deteriorated glass samples are all covered with a weathering crust and numerous small and large craters are observed with SEM (scanning electron microscopy). The crust is rather powdery and can be easily scraped off. Fig. 8 shows a secondary electron image of a crater on the glass surface. The crystalline products with a plate-like structure in and around the crater can be characterized as gypsum ($CaSO_4 \cdot 2H_2O$).[13] EPXMA studies of the weathering crust reveal that the products mainly consist of calcium and sulfur. Far-IR measurements of the white powder present on the surface and in the craters confirm this statement.

The actual condition of medieval glass depends on the chemical composition of the bulk glass. Glasses with high potash and low silica content will have a severely crusted surface while a higher silica content will lead to corrosion by pitting. Nevertheless, other parameters, such as the environmental conditions and the manufacturing process of the glass, can play an important role.[14]

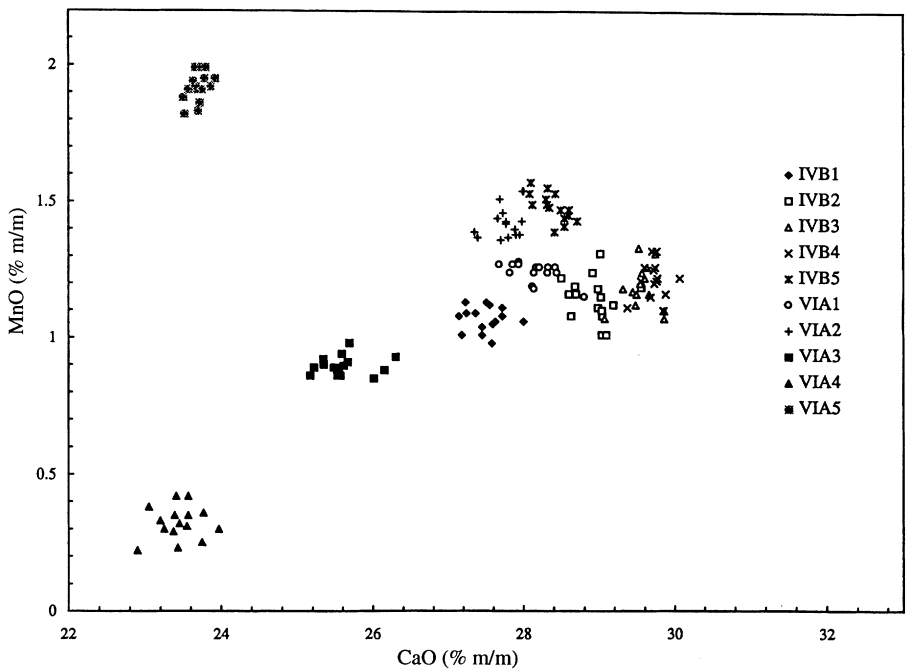

Fig. 7 Ca–Mn plot showing three outliers among the ten measured glass panels from Brussels' Cathedral.

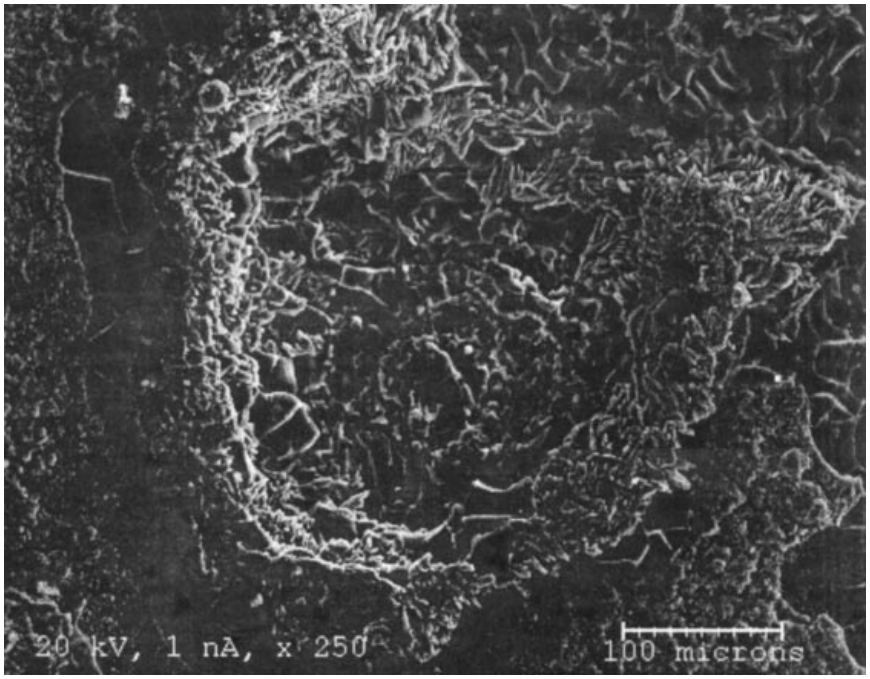

Fig. 8 Secondary electron image of gypsum formed in and around a crater on the pitted and crusted surface.

Surface Patina on Buried Nephrite Objects

Jade (nephrite) artefacts from burial sites of the Han dynasty in China are commonly covered with a white powdery layer on parts of the objects. Several explanations have been proposed regarding the origin of this particular surface layer, either explaining it as (i) an organic deposit from decomposing bodies or other objects in the grave or (ii) as a calcification of the jade objects or finally (iii) as due to leaching of the mineral in the medium of decomposing bodies. As shown in Table 6, electron microanalysis of the altered surface layers on some of the objects shows readily that the surface layer has the same composition as the nephrite from which it originates. This clearly points to an alteration process of the jade objects under the influence of the alkaline medium of decomposing human bodies. This explanation has been advanced earlier by Gaines and Handy in 1975.[15] Hence, the process occurs during the first few months after burial and the alteration layer cannot be used to prove that an object has been buried for a long period of time. The regions of alteration are correlated with the surface state of the objects as it occurs most often on unpolished or mineralogically weaker parts of the objects.[16]

PIGMENT ANALYSIS OF GLASS PAINTINGS[17]

One of the methods of colouring glass is to cover a colourless glass pane with a thin layer of paint; two types exist: grisailles and enamels. The grisaille paint consists of a flux (*e.g.*, a crystal glass of $4PbO \cdot 5SiO_2$) and a pigment (*e.g.*, Fe_2O_3). The mixture is ground, painted onto the glass and fired at approximately 630 °C in order to fuse it to the surface (Fig. 9). In contrast, an enamel is a coloured glass with a low melting-point (*e.g.*, Fe_2O_3–PbO–SiO_2). It consists of one type of grain and gives after firing a more homogeneous paint layer than a grisaille (Fig. 10).

The glass paint Rouge Jean Cousin is a collective name for all the paints with a carnation red colour used for colouring heads, hands and bodies on stained glass windows. This type of paint was used from the fifteenth century until the beginning of the twentieth century. In the nineteenth century the name Rouge Jean Cousin was given to the carnation red paints after their presumed discoverer Jean Cousin the elder (1490–1560) or Jean Cousin the younger (1522–1594). A study of these carnation red glass paints was performed at MiTAC by analysing historical stained glass windows and Rouge Jean Cousin

Table 6 Comparison of composition of bulk nephrite and three deposit layers.* All values in % m/m

Oxides	Nephrite: Literature	Nephrite: Electron microscopy	Deposit: Sample A†	Deposit: Sample B‡	Deposit: Sample C§
Na_2O	1.3	—	—	—	—
MgO	24.2	21.5±0.2	24.4±2.3	23.7±2.7	25.2±2.4
Al_2O_3	1.3	0.7±0.1	1.1±0.5	1.1±0.7	0.9±0.6
SiO_2	58.0	57.5±0.3	60.2±0.6	60.3±1.0	60.3±0.7
P_2O_5	—	0.1±0.1	0.1±0.1	0.2±0.2	0.1±0.1
SO_3	—	0.9±0.1	0.3±0.1	0.1±0.1	0.1±0.1
Cl	—	0.2±0.1	0.4±0.2	0.1±0.1	0.1±0.1
K_2O	—	0.9±0.1	0.3±0.2	0.1±0.1	0.2±0.1
CaO	13.2	13.7±0.1	12.2±1.7	13.3±2.1	12.5±2.0
FeO	2.1	4.5±0.1	1.1±0.4	1.0±0.3	0.7±0.3

* Chemical analysis of polished nephrite and of the deposit of three samples from the Dongxi Collection, Brussels, compared with the average composition of nephrite.

† Sample A: Huang with whorl pattern, Late Spring and Autumn period, 6th/5th century BC.

‡ Sample B: Green and brown congé with flat walls, Zhou period, *c.* 1050–256 BC.

§ Sample C: Small round disc in the form of an animal, Late Zhou–early Western Han dynasty, 3rd/2nd century BC.

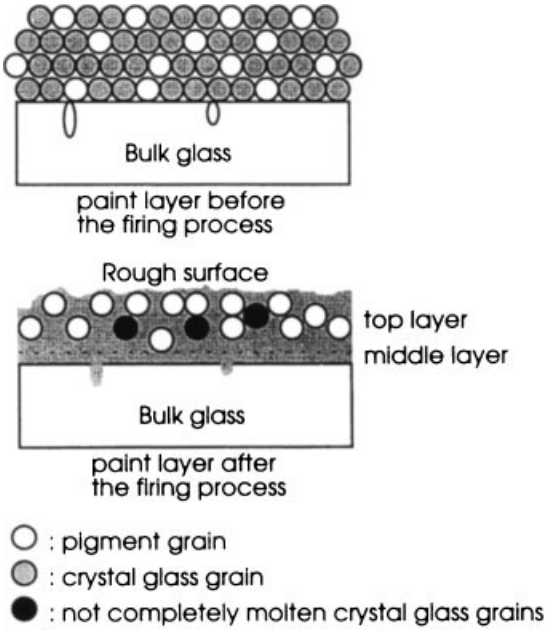

Fig. 9 Schematic diagram of a grisaille paint layer.

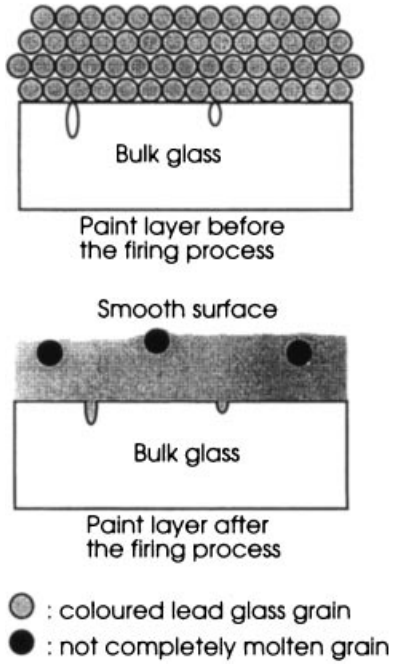

Fig. 10 Schematic diagram of an enamel paint layer.

powders and the results were compared with recipes found in the literature from the seventeenth to the nineteenth century.

This carnation red paint exists as a grisaille in the period between the fifteenth and the beginning of the nineteenth century. A red grisaille was obtained when Fe_2O_3 grains with a particle size smaller then 0.5 μm were used and when the paint layer had a thickness of about 1 μm. These small pigment grains were collected by mixing pigment, flux and arabic gum in a glass of water. The largest particles sank to the bottom after 3–5 d. The upper part, containing the smallest particles, was decanted and evaporated to obtain the red paint.

At the end of the nineteenth century, glass paints were produced industrially by Lacroix & Cie in Paris (France) and Kielblock in Arnstadt (Germany) for example. The analysis of Rouge Jean Cousin powders of Lacroix and Kielblock reveals that these paints are enamels, because a single grain contained

Table 7 Average composition of Rouge Jean Cousin particles of Lacroix (% m/m) as determined with SEM

Oxide	Composition determined with EPXMA	Composition calculated from the recipe
B_2O_3	Present	6.25
Na_2O	3.00 ± 0.4	2.79
MgO	0.91 ± 0.05	—
Al_2O_3	2.9 ± 0.10	—
SiO_2	17.11 ± 0.60	16.95
K_2O	0.41 ± 0.05	—
CaO	2.30 ± 0.3	—
Fe_2O_3	34.3 ± 0.5	19.70
CuO	0.38 ± 0.07	—
ZnO	0.29 ± 0.04	—
PbO	38.4 ± 0.7	54.31

SiO_2, PbO and Fe_2O_3 at the same time, which indicates that pigment and glass were melted together and ground afterwards. Table 7 shows the average composition of the Rouge Jean Cousin powders of Lacroix and the composition calculated from the original recipe of Lacroix. The two are not the same, but there is a resemblance.

In conclusion, a change in production of carnation red glass paints from grisaille to enamel paints seems to have taken place at the end of the nineteenth century.

CONCLUSIONS

All these examples from our laboratory's projects were selected with the aim of showing the potential of instrumental analytical techniques in archaeology and art.

The kind of applications discussed in this paper are multidisciplinary *par excellence*. In the first place they rely heavily on the experience of the laboratory in the field of environmental analysis as the corrosion of buried objects often critically depends on the local environment from which they are recovered. Second, the characterization of archaeological and art objects poses similar problems of sample handling and analytical procedures as that of modern technological materials. Finally, this type of work is extremely specialized and multidisciplinary with a necessity of collaboration between analytical chemistry and various other disciplines (history, art history, restoration, archaeology, *etc.*). In such circumstances, collaboration with specialized institutes is mandatory. In the examples given in this paper we worked in collaboration with the Oriental Institute of the University of Chicago for the early tin metallurgy, with the Royal Academy of Fine Arts (Antwerp), the National Institute for the Cultural Heritage (Brussels) and the Fraunhofer Institut für Silicatenforschung (Würzburg) for the glass corrosion, and with several art collectors and art historians for the other problems discussed.

The authors thank K. A. Yener (Oriental Institute, Chicago), H. Özbal (Bogazici University, Istanbul), B. Earl (Cornwall), N. Van Hout, A. Balis (Rubenianum, Antwerpen), H. Wouters (Royal Institute for Cultural Heritage, Brussels) and J. Caen (Royal Academy of Fine Arts) for the samples and interesting discussions. We are also indebted to L. d'Alessandro, L. Vincze and P. Veny who assisted in the analysis of the trace elements and to C. Yang, R. Utui and K. Malmqvist for assistance with the μ-PIXE measurements.

REFERENCES

1 Yener, K. A., Özbal, H., Kaptan, E., Pehlivan, A. N., and Goodway, M., *Science*, 1989, **244**, 200.
2 Yener, K. A., and Vandiver, P., *Am. J. Archeol.*, 1993, **97**, 207.
3 Earl, B.,and Özbal, H., *Archaeometry*, 1996, **38**, 289.

4 Bachmann, H., *The Identification of Slags from Archaeological Sites*, Institute of Archaeology, London, 1982.
5 Adriaens, A., *Mikrochim. Acta*, 1996, **124**, 89.
6 Yener, K. A., *The Göltepe/Kestel Project: 1994–1995 Annual Report*, Oriental Institute, Chicago, IL, 1996.
7 Turner, W. E. S., *J. Soc. Glass Technol*., 1956, **XL**, 194 and 277.
8 Donceel-Voûte, P., *Archeologia*, 1994, **98**, 24.
9 Geilmann, W., *Glastech. Ber*., 1956, **29**, 145.
10 Caen, J., *Art Restorers Assoc*., 1993, 9.
11 Berckmans, W., *Research Report*, Royal Academy for Fine Arts, Antwerp, 1990.
12 Genicot, F.-F., and Coomans, T., *Revue des Archéologues et Historiens d'art de Louvain*, 1992, 11.
13 Gillies, K. J. S., and Cox, A., *Glastech. Ber*., 1988, **61**, 75.
14 Schreiner, M., *Glastech. Ber*., 1988, **61**, 197.
15 Gaines, A. M., and Handy, J. L., *Nature (London)*, 1975, **253**, 433.
16 Aerts, A., Janssens, K., and Adams, F., *Orientations*, 1995, 79.
17 Schalm, O., Janssens, K., Albert, J., Peeters, K., Caen, J., and Adams, F., in *Dossier de la Commision Royale de Monuments, Sites et Fouilles, Proceedings of Forum pour la Conservation et la restauration des Vitraux, Liège, June 19–22, 1996*, ed. Barlet, J., Commission Royale des Monuments, Sites et Fouilles, Liège, Belgium, 1996, vol. 3, pp. 155–162.

Paper 6/06091I
Received September 9, 1996
Accepted January 6, 1997